Transmission expansion planning including TCSCs and SFCLs: A MINLP approach

M. Esmaili, *Senior Member, IEEE*, M. Ghamsari-Yazdel, *Student Member, IEEE*, N. Amjady, *Senior Member, IEEE*, C. Y. Chung, *Fellow, IEEE*, A. J. Conejo, *Fellow, IEEE*

***Abstract* — We propose a transmission expansion planning model that integrates thyristor-controlled series compensators (TCSCs) to enhance line transmission capacity, and superconducting fault current limiters (SFCLs) to control short-circuit levels. The harmonious interplay between TCSCs and SFCLs results in effective and economically attractive optimal expansion plans. This multi-stage planning model translates into a complex mixed-integer nonlinear programming problem, which is hard to solve. To solve it, we propose a successive linearization technique within a Benders' decomposition scheme that proves effective in finding optimal solutions and efficient in terms of computational burden. We illustrate the methodology proposed using the IEEE 39-bus system.**

***Index terms* — Transmission expansion planning, superconducting fault current limiter (SFCL), short circuit level, thyristor-controlled series compensator (TCSC), Benders' decomposition.**

NOMENCLATURE

Sets and Indices

$l \in \Omega_{LC}, \Omega_L$	Index and sets for candidate and all lines, respectively.
$g \in \Omega_G$	Index and set for generators.
$r \in \Omega_r$	Index and set for resistive SFCL modules.
$x \in \Omega_x$	Index and set for inductive SFCL modules.
$t \in \Omega_T$	Index and set for planning periods (years).
$i, j, m, n \in \Omega_N$	Indices and set for buses.
$d \in \Omega_D$	Index and set for demand levels obtained from clustering of hourly load demands.
$q \in \Omega_Q$	Index and set for maximum TCSC compensation level.

Superscript

Re, Im	Real and imaginary parts of complex-valued quantities.

Parameters

γ	Discount rate of investment.
IC_l^{LC}	Investment cost for candidate line l.
$IC_{l,q}^T$	Investment cost for a TCSC with a maximum of q compensation levels at line l.
$IC_{l,r}^{LSR}/IC_{l,x}^{LSX}$	Investment cost for a resistive/inductive SFCL with r/x modules at line l.
$IC_{g,r}^{GSR}/IC_{g,x}^{GSX}$	Investment cost for a resistive/inductive SFCL with r/x modules at generator g.
G_l^L, B_l^L	Conductance & susceptance of line l.
$G_{l,q}^{min}$,$B_{l,q}^{min}$	Minimum parallel equivalent conductance & susceptance resulting from a TCSC with a maximum of q compensation levels at line l.
$G_{l,q}^{max}$, $B_{l,q}^{max}$	Maximum parallel equivalent conductance & susceptance resulting from a TCSC with a maximum of q compensation levels at line l.
$G_{l,r}^{PLSR}$, $B_{l,r}^{PLSR}$	Parallel equivalent conductance & susceptance resulting from a series resistive SFCL with r modules at line l.
$G_{l,x}^{PLSX}$, $B_{l,x}^{PLSX}$	Parallel equivalent conductance & susceptance resulting from a series inductive SFCL with x modules at line l.
$G_{g,r}^{PGSR}$, $B_{g,r}^{PGSR}$	Parallel equivalent conductance & susceptance resulting from a resistive SFCL with r modules at generator g.
$G_{g,x}^{PGSX}$, $B_{g,x}^{PGSX}$	Parallel equivalent conductance & susceptance resulting from an inductive SFCL with x modules at generator g.
S_l^L	Maximum apparent power of line l.
$S_{l,q}^T$	Increment in the maximum apparent power of line l due to installing a TCSC with a maximum of q compensation levels.
$\varpi_{l,i,j}$	1 if line l connects buses i and j; 0 otherwise.
$\mathcal{N}_{g,i}$	1 if generator g is at bus i; 0 otherwise.
$P_{i,d,t}^D$, $Q_{i,d,t}^D$	Active and reactive loads of bus i at demand level d and time period t.
π_t	Value of energy losses at period t.
τ_d	Duration of demand level d.
C_g^{OP}	Operation cost of generator g.
P_g^{Gmin}, P_g^{Gmax}	Limits on active power of generator g.
Q_g^{Gmin}, Q_g^{Gmax}	Limits on reactive power of generator g.
V_i^{min} , V_i^{max}	Limits on voltage magnitude of bus i.
$Z_i^{0,Re}$, $Z_i^{0,Im}$	Diagonal element i of the original impedance matrix.
$I_i^{SC,max}$	Allowable short circuit level at bus i.

Variables

$\varphi_{l,t}$	1 if line l is planned at time t; 0 otherwise.
$\psi_{l,q,t}$	1 if a TCSC with a maximum of q compensation levels is planned in line l at time t; 0 otherwise.
$e_{l,r,t}/f_{l,x,t}$	1 if a resistive/inductive SFCL with r/x modules is planned in line l at time t; 0 otherwise.

M. Esmaili (corresponding author) and C. Y. Chung are with the Department of Electrical and Computer Engineering, University of Saskatchewan, Saskatoon, SK S7N 5A9 Canada (E-mail: msdesmaili@gmail.com, c.y.chung@usask.ca).

M. Ghamsari-Yazdel is with the Department of Electrical Engineering, West Tehran Branch, IAU, Tehran, Iran E-mail: ghamsari@birjand.ac.ir).

N. Amjady is with the Department of Electrical and Computer Engineering, Semnan University, Semnan, Iran (E-mail: amjady@semnan.ac.ir).

Antonio J. Conejo is with Department of Integrated Systems Engineering and the Department of Electrical and Computer Engineering, The Ohio State University, Columbus, OH 43210, USA (E-mail: conejo.1@osu.edu).

$v_{g,r,t}/w_{g,x,t}$ — 1 if a resistive/inductive SFCL with r/x modules is planned in generator g at time t; 0 otherwise.

$G^{PT}_{l,d,t}$, $B^{PT}_{l,d,t}$ — Parallel equivalent conductance & susceptance resulting from a TCSC in line l at demand level d and period t.

$G^{PLS}_{i,j,t}$, $B^{PLS}_{i,j,t}$ — Parallel equivalent conductance & susceptance added to corridor ij due to a line series SFCL.

$G^{PGS}_{i,t}$, $B^{PGS}_{i,t}$ — Parallel equivalent conductance & susceptance added to bus i due to a generator series SFCL.

$G^{CN}_{i,j,d,t}$, $B^{CN}_{i,j,d,t}$ — Corridor ij conductance & susceptance at demand level d and period t in normal operation.

$G^{CF}_{i,j,t}$, $B^{CF}_{i,j,t}$ — Incremental conductance & susceptance of corridor ij in faulted condition at period t due to adding lines, TCSCs, and line SFCLs.

$P^{G}_{g,d,t}$, $Q^{G}_{g,d,t}$ — Active & reactive power outputs of generator g at demand level d and period t.

$P^{C}_{i,j,d,t}$, $Q^{C}_{i,j,d,t}$ — Active & reactive power flows from bus i to j through existing & candidate lines at demand level d and period t.

$V_{i,d,t}$, $\delta_{i,d,t}$ — Magnitude and angle of bus i voltage at demand level d and period t.

$S^{max}_{i,j,t}$ — Dynamic maximum apparent power of corridor ij at period t.

$P^{Loss}_{d,t}$ — Power losses at demand level d and period t.

$\Delta Z^{L,Im}_{i,m,n,t}$ — Change in diagonal element i of Z_{BUS} at period t due to adding new components (i.e., lines, TCSCs, and SFCLs) to corridor mn.

$\Delta Z^{G,Im}_{i,m,t}$ — Change in diagonal element i of Z_{BUS} at period t due to adding generator SFCLs at bus m.

$Z^{Im}_{i,t}$ — Diagonal element i of Z_{BUS} at period t.

$I^{SC}_{i,d,t}$ — Short circuit level of bus i at demand level d and period t.

I. Introduction

A. Motivation and Background

Transmission expansion planning (TEP) is carried out to meet transmission network requirements to supply the future load of power systems. Additionally, thyristor-controlled series compensators (TCSCs) are employed to improve the power transfer capability of existing lines, voltage stability, and operation flexibility [1]. The TCSC technology is mature with many installations across the globe [2]. However, when prospective transmission lines/TCSCs are added to an existing power system, they increase the short circuit (SC) level of existing substations by lowering transmission impedances [3]. Such an increase in SC levels may violate allowable limits. One solution is to upgrade the SC level of existing substation components, such as switchgears and transformers, a task that entails high costs of construction and power interruptions during the upgrading process. An alternative approach is to enforce the SC limits in the planning stage to achieve a cost-effective and practical solution. However, a SC-constrained planning model may result in either building a smaller number of candidate lines or building low capacity/high impedance lines to keep the SC level under limits. This implies that the optimal solution of the SC-constrained planning model may be biased.

Superconducting fault current limiters (SFCLs) have recently called the attention of power system planners due to their capabilities in efficiently mitigating fault currents. Some instances have been installed in the USA, Europe, Asia, and UK [4]. SFCLs are invisible in normal operation since they introduce nearly zero series impedances; however, they quickly exhibit large impedances in fault conditions to limit SC currents [5]. They can also help mitigate transient stability issues by limiting the amount of kinetic energy absorbed by the power system during the fault-on period. SFCLs are available in the market as resistive, inductive, or hybrid types [5], [6]. Using SFCLs allows building high-capacity lines with or without TCSCs while keeping the SC levels within allowable limits. Since SFCLs are rather expensive, SFCL optimal placement (SOP) is performed to effectively employ the least number of SFCLs. In addition, as TEP, TCSC allocation, and SFCL placement are planning issues, it will be practical to jointly address the three of them.

Dynamic TEP (with time-dependent expansion decisions) is a hard-to-solve mixed-integer nonlinear programming (MINLP) problem if an AC network model is used [7]. The inclusion of TCSCs and SFCLs in the dynamic AC TEP makes it more challenging due to turning line admittances and network impedance matrix (Z_{BUS}) elements into variables. Therefore, appropriate linearization methods are needed to convert the MINLP problem into a mixed-integer linear programming (MILP) with acceptable linearization errors. There are some linearization techniques available in the literature, such as [8], [9], [10]. However, they are not valid if transmission corridor impedances are variables.

B. Literature Review

The joint planning of TCSCs and lines is addressed in [1] as an MINLP problem; however, a DC network model is employed. On the other hand, fault currents have been considered in TEP in a limited number of works. In [3] and [11], the SC-constrained TEP is formulated as an MILP problem, where a DC network model is used. Thus, the model cannot be used to determine optimal resistive/inductive SFCL modules. Although SC levels are restricted in [12] by SFCLs, its power system model does not consider admittance matrix changes. In [13] a SC-constrained system expansion planning model is presented considering bundling and voltage levels of lines.

Depending on a number of parameters, including the network X/R ratios and the load power factors, the combination of resistive/inductive SFCL that best matches a branch or generator can be determined. However, most SOP works assume a purely resistive or inductive SFCL. For instance, resistive SFCLs are optimally placed in [5] and [14] using a sensitivity analysis pertaining to transient stability. In [15], although SOP is addressed using a genetic algorithm, complex-valued SFCLs are not modeled. A SOP is proposed in [16] using an iterative technique, where an inductive SFCL is installed at each iteration to evade a variable Z_{BUS}. SFCL locations and sizes at previous iterations are assumed fixed for the current iteration. This technique does not allocate all SFCLs simultaneously. In [17], a two-stage SOP is proposed. In the first stage, the optimal locations of SFCLs are obtained to reduce the search space, whereas in the second stage, the optimal sizes of SFCLs are determined. In [18], hybrid SFCLs are optimally placed. However, Z_{BUS} updating, a key feature in SOP, is not modeled. Moreover, since the number of SFCLs is not optimized in [18], a very high number of SFCLs may be placed.

Generalized Benders' decomposition is used in the literature to decompose an MINLP problem into an MILP master problem (MP) and a nonlinear programming (NLP) subproblem (SP) [19]. However, only in the case of a convex NLP, it is possible to guarantee that the global optimal solution is attained [20]. To this end, some works linearize the nonlinear SP to achieve convexity. For instance, nonlinear power flow equations in the SP are linearized in [21]; however, linearization errors are not considered, and a high linearization error may lead to a non-optimal solution. In some works, such as [22], the power flow equations are convexified via relaxation. However, these convex models can only be used if branch impedances are constant. To achieve an optimal solution, we propose a modified Benders decomposition (BD) scheme in which the linearization errors approach zero through re-linearization over the iterations.

C. Contributions and the Organization of the Paper

In light of the literature review, the contributions of this paper can be summarized as:

- Joint planning of transmission lines and TCSCs considering SC limits. For some transmission corridors, installing TCSCs may provide more cost-effective solution than adding new lines.
- Optimal siting of hybrid SFCLs to control SC levels that may increase as a result of adding new lines and TCSCs. This allows planning high capacity lines with low impedances and low energy losses. In addition, the costly upgrading of existing substations to reinforce their SC levels is avoided.
- Proposing a novel BD scheme to solve the considered MINLP problem. Nonlinear functions are re-linearized over BD iterations to minimize linearization errors. Upon convergence, the solution obtained by the linearized problem matches that of the MINLP model due to zero linearization errors.

These contributions fill some research gaps in TEP and they are specific to this paper. It is worthwhile to note that although distributed generations (DGs) may be able to reduce burden of transmission systems by locally producing power, they are not included in this paper. Its reason is that planning of DGs is performed at distribution level [8] with the outcome of distribution future power requirements as an input to the TEP.

The rest of this paper is organized as follows. In Section II, the effects of adding candidate lines, TCSCs, and SFCLs on the Z_{BUS} are analyzed. In Section III, the proposed MINLP model is presented and linearized. The re-linearization-based BD scheme is presented in Section IV. Section VI presents case studies and their discussions. Finally, Section VII concludes the article.

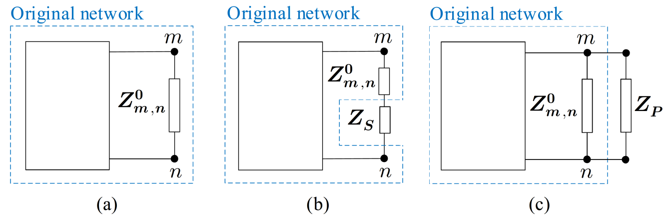

Fig. 1. Addition of a series impedance to the network, (a) original network, (b) added series impedance, (c) equivalent parallel impedance.

II. The Effects of Adding New Lines, TCSCs, and SFCLs on the Network Impedance Matrix

A. The Effect of Adding an Impedance in Series with a Branch

A branch with impedance $\boldsymbol{Z^0_{m,n}}$ (bold fonts are used for complex-valued quantities) between buses m and n is shown in Fig. 1(a). An impedance $\boldsymbol{Z_S}$ is connected in series with this branch in Fig. 1(b). Then, the series impedance is converted to its parallel equivalent impedance $\boldsymbol{Z_P}$ in Fig. 1(c). To obtain the value of $\boldsymbol{Z_P}$, the resulting equivalent impedances in Fig. 1(b) and Fig. 1(c) should be the same: $\boldsymbol{Z^0_{m,n}} + \boldsymbol{Z_S} = \boldsymbol{Z^0_{m,n}} \parallel \boldsymbol{Z_P}$. By solving this equation for $\boldsymbol{Z_P}$, we obtain:

$$\boldsymbol{Z_P} = \frac{\boldsymbol{Z^0_{m,n}}(\boldsymbol{Z_S} + \boldsymbol{Z^0_{m,n}})}{-\boldsymbol{Z_S}}\ . \tag{1}$$

The Thevenin equivalent impedance as seen from bus i is the corresponding diagonal element of Z_{BUS} ($\boldsymbol{Z_{i,i}}$) [23]. We consider a 3-phase fault since it usually results in the worst case SC current as compared with other types of faults [23]. The SC level at bus i is calculated as $\boldsymbol{V_i}/\boldsymbol{Z_{i,i}}$, where $\boldsymbol{V_i}$ is the voltage at bus i. As a result of adding $\boldsymbol{Z_P}$ between buses m and n, the change in the diagonal element ii of Z_{BUS} is expressed as [23]:

$$\Delta \boldsymbol{Z_{i,i}} = \frac{-(\boldsymbol{Z^0_{i,m}} - \boldsymbol{Z^0_{i,n}})^2}{\boldsymbol{Z^0_{m,m}} + \boldsymbol{Z^0_{n,n}} - 2\boldsymbol{Z^0_{m,n}} + \boldsymbol{Z_P}} \tag{2}$$

where $\boldsymbol{Z^0_{i,j}}$ $(\forall i, j)$ represents the original element ij of Z_{BUS} (before adding a new component). Since the added component is parallel in Fig. 1(c), it is convenient to express it in term of its admittance $\boldsymbol{Y_P} = \boldsymbol{1}/\boldsymbol{Z_P}$. By substituting $\boldsymbol{Z_P}$ from (1) into (2) and expressing it in terms of $\boldsymbol{Y_P}$, we obtain:

$$\Delta \boldsymbol{Z_{i,i}} = \frac{-(\boldsymbol{Z^0_{i,m}} - \boldsymbol{Z^0_{i,n}})^2 \boldsymbol{Y_P}}{1 + (\boldsymbol{Z^0_{m,m}} + \boldsymbol{Z^0_{n,n}} - 2\boldsymbol{Z^0_{m,n}})\boldsymbol{Y_P}} \tag{3}$$

B. The Effect of Adding Lines, TCSCs, and Line SFCLs

A TCSC/SFCL is placed in series with an existing/new line as shown in Fig. 2(a). The original Z_{BUS} diagonal elements are changed as a result of adding line-related components, which can be converted into their parallel equivalent admittances as shown in Fig. 2(b). For instance, the impact of adding an SFCL to the existing line mn ($\boldsymbol{Y^{PLS}_{L1}}$) on diagonal elements of Z_{BUS} can be written from (3) as:

$$\Delta \boldsymbol{Z^{L}_{i,m,n}} = \frac{-(\boldsymbol{Z^0_{i,m}} - \boldsymbol{Z^0_{i,n}})^2 \boldsymbol{Y^{PLS}_{L1}}}{1 + (\boldsymbol{Z^0_{m,m}} + \boldsymbol{Z^0_{n,n}} - 2\boldsymbol{Z^0_{m,n}})\boldsymbol{Y^{PLS}_{L1}}} \tag{4}$$

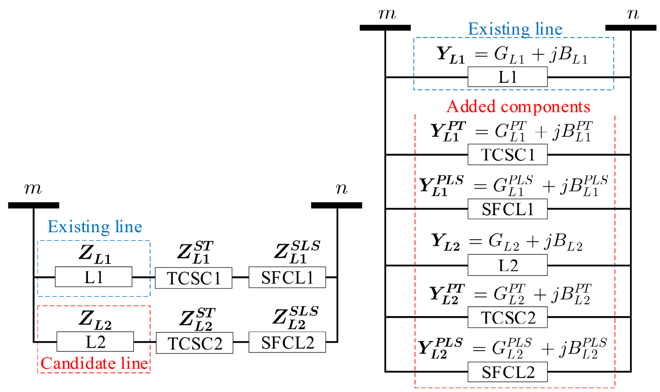

(a) (b)

Fig. 2. Existing and candidate lines with SFCL and TCSC, (a) series connection, (b) equivalent parallel connection.

where $\Delta Z^{L}_{i,m,n}$ represents the change in diagonal element i of ZBUS due to adding $\boldsymbol{Y^{PLS}_{L1}}$. Since elements of the original ZBUS are constants, it is possible to simplify (4) by defining the constants $\boldsymbol{A_{i,m,n}} = -(\boldsymbol{Z^{0}_{i,m}} - \boldsymbol{Z^{0}_{i,n}})(\boldsymbol{Z^{0}_{m,i}} - \boldsymbol{Z^{0}_{n,i}})$ and $\boldsymbol{B_{m,n}} = (\boldsymbol{Z^{0}_{m,m}} + \boldsymbol{Z^{0}_{n,n}} - 2\boldsymbol{Z^{0}_{m,n}})$ as:

$$\Delta \boldsymbol{Z^{L}_{i,m,n}} = \frac{\boldsymbol{A_{i,m,n}}.\boldsymbol{Y^{PLS}_{L1}}}{1+\boldsymbol{B_{m,n}}.\boldsymbol{Y^{PLS}_{L1}}} \quad . \tag{5}$$

Although (5) is derived to provide the effect of adding SFCL1 to an existing line on the diagonal elements of ZBUS, it can be similarly used for other parallel components in Fig. 2(b) (namely, TCSC1, line L2, TCSC2, and SFCL2). All added components become parallel components in Fig. 2(b) once they are converted to their equivalent parallel admittances. By summing up all parallel admittances of added components, the change in the diagonal element i of ZBUS is calculated as:

$$\Delta \boldsymbol{Z^{L}_{i,m,n}} = \frac{\boldsymbol{A_{i,m,n}}(\boldsymbol{Y^{PLS}_{L1}}+\boldsymbol{Y^{PT}_{L1}}+\boldsymbol{Y_{L2}}+\boldsymbol{Y^{PLS}_{L2}}+\boldsymbol{Y^{PT}_{L2}})}{1+\boldsymbol{B_{m,n}}(\boldsymbol{Y^{PLS}_{L1}}+\boldsymbol{Y^{PT}_{L1}}+\boldsymbol{Y_{L2}}+\boldsymbol{Y^{PLS}_{L2}}+\boldsymbol{Y^{PT}_{L2}})} \, . \tag{6}$$

where superscript $^{\boldsymbol{L}}$ denotes the changes as a result of adding the line-related components. In fact, all changes due to adding new components are merged in (6) and are applied to the original ZBUS elements only once. This type of one-step ZBUS updating, rather than updating repeatedly, reduces the number of constraints of the optimization problem. Equation (6) can be rewritten using real and imaginary parts as:

$$\begin{aligned}&\Delta Z^{L,Re}_{i,m,n} + j\Delta Z^{L,Im}_{i,m,n} \\ &= \frac{(A^{Re}_{i,m,n}+jA^{Im}_{i,m,n})(G^{CF}_{m,n}+jB^{CF}_{m,n})}{1+(B^{Re}_{m,n}+jB^{Im}_{m,n})(G^{CF}_{m,n}+jB^{CF}_{m,n})}\end{aligned} \tag{7}$$

where $G^{CF}_{m,n} = G^{PLS}_{L1} + G^{PT}_{L1} + G_{L2} + G^{PLS}_{L2} + G^{PT}_{L2}$ and $B^{CF}_{m,n} = B^{PLS}_{L1} + B^{PT}_{L1} + B_{L2} + B^{PLS}_{L2} + B^{PT}_{L2}$, as their components are shown in Fig. 2(b), represent the total parallel conductance and susceptance of the new components.

C. The Effect of Adding Generator SFCLs

A series generator SFCL with impedance $\boldsymbol{Z^{SGS}_{m}}$ at bus m can be represented by an equivalent parallel admittance $\boldsymbol{Y^{PGS}_{m}}$ [23]:

$$\boldsymbol{Y^{PGS}_{m}} = -\frac{\boldsymbol{Z^{SGS}_{m}}}{\boldsymbol{Z^{G0}_{m}}(\boldsymbol{Z^{G0}_{m}}+\boldsymbol{Z^{SGS}_{m}})} \tag{8}$$

where $\boldsymbol{Z^{G0}_{m}}$ is the generator impedance. The change in ZBUS is [23]:

$$\Delta \boldsymbol{Z^{G}_{i,m}} = -\frac{(\boldsymbol{Z^{0}_{i,m}})^{\boldsymbol{2}}}{1+\boldsymbol{Z^{0}_{m,m}}\boldsymbol{Y^{PGS}_{m}}} \tag{9}$$

where $\Delta \boldsymbol{Z^{G}_{i,m}}$ represents the change in the diagonal element i of ZBUS due to $\boldsymbol{Y^{PGS}_{m}}$. By defining constants $\boldsymbol{C_{i,m}} = -(\boldsymbol{Z^{0}_{i,m}})^{\boldsymbol{2}}$ and $\boldsymbol{D_{m}} = \boldsymbol{Z^{0}_{m,m}}$, (9) is simplified as:

$$\Delta \boldsymbol{Z^{G}_{i,m}} = \frac{\boldsymbol{C_{i,m}}}{1+\boldsymbol{D_{m}}\boldsymbol{Y^{PGS}_{m}}} \tag{10}$$

where $\boldsymbol{C_{i,m}}$ and $\boldsymbol{D_{m}}$ can be calculated from the original ZBUS. Rewriting complex-valued quantities in (10) using their real and imaginary parts yields:

$$\begin{aligned}&\Delta Z^{G,Re}_{i,m} + j\Delta Z^{G,Im}_{i,m} \\ &= \frac{C^{Re}_{i,m}+jC^{Im}_{i,m}}{1+(D^{Re}_{m}+jD^{Im}_{m})(G^{PGS}_{m}+jB^{PGS}_{m})} \quad .\end{aligned} \tag{11}$$

III. Proposed Model for TEP with TCSCs and SFCLs

In this section, the MINLP model is explained first. Then, the model is linearized to improve its tractability.

A. MINLP Model

The objective function of the proposed MINLP model of TEP with TCSC and SFCL is:

$$\min_{\varphi,\psi,e,f,v,w,P^G,Q^G} C = C_I + C_{OP} \tag{12}$$

where the investment cost C_I and the operation cost C_{OP} are as follows:

$$\begin{aligned}C_I = &\sum_{\forall t, l\in\Omega_{LC}} \frac{IC^{LC}_{l}(\varphi_{l,t}-\varphi_{l,t-1})}{(1+\gamma)^{t-1}} + \sum_{\forall l,q,t} \frac{IC^{T}_{l,q}(\psi_{l,q,t}-\psi_{l,q,t-1})}{(1+\gamma)^{t-1}} \\ &+ \sum_{\forall l,r,t} \frac{IC^{LSR}_{l,r}(e_{l,r,t}-e_{l,r,t-1})}{(1+\gamma)^{t-1}} + \sum_{\forall l,x,t} \frac{IC^{LSX}_{l,x}(f_{l,x,t}-f_{l,x,t-1})}{(1+\gamma)^{t-1}} + \\ &\sum_{\forall g,r,t} \frac{IC^{GSR}_{g,r}(v_{g,r,t}-v_{g,r,t-1})}{(1+\gamma)^{t-1}} + \sum_{\forall g,x,t} \frac{IC^{GSX}_{g,x}(w_{g,x,t}-w_{g,x,t-1})}{(1+\gamma)^{t-1}}\end{aligned} \tag{13}$$

$$C_{OP} = \sum_{\forall g,d,t} \frac{P^{G}_{g,d,t}C^{OP}_{g}\tau_d}{(1+\gamma)^{t-1}} + \sum_{\forall d,t} \frac{\pi_t P^{Loss}_{d,t}\tau_d}{(1+\gamma)^{t-1}} \tag{14}$$

The constraints of the proposed MINLP model of TEP with TCSC and SFCL are (15)-(50).

Normal operation (added new lines and TCSCs):

$$\varphi_{l,t} \geq \varphi_{l,t-1} \tag{15}$$

$$\psi_{l,q,t} \geq \psi_{l,q,t-1} \tag{16}$$

$$\sum_{\forall q} \psi_{l,q,t} \leq \varphi_{l,t} \tag{17}$$

$$\sum_{\forall q} G^{min}_{l,q}\psi_{l,q,t} \leq G^{PT}_{l,d,t} \leq \sum_{\forall q} G^{max}_{l,q}\psi_{l,q,t} \tag{18}$$

$$\sum_{\forall q} B^{min}_{l,q}\psi_{l,q,t} \leq B^{PT}_{l,d,t} \leq \sum_{\forall q} B^{max}_{l,q}\psi_{l,q,t} \tag{19}$$

$$G^{CN}_{i,j,d,t} = \sum_{\forall l} G^L_l \varphi_{l,t}\varpi_{l,i,j} + \sum_{\forall l} G^{PT}_{l,d,t}\varpi_{l,i,j} \tag{20}$$

$$B^{CN}_{i,j,d,t} = \sum_{\forall l} B^L_l \varphi_{l,t}\varpi_{l,i,j} + \sum_{\forall l} B^{PT}_{l,d,t}\varpi_{l,i,j} \tag{21}$$

$$S^{max}_{i,j,t} = \sum_{\forall l} \varphi_{l,t} S^L_l \varpi_{l,i,j} + \sum_{\forall l,q} \psi_{l,q,t} S^T_{l,q}\varpi_{l,i,j} \tag{22}$$

$$P^{Loss}_{d,t} = \sum_{\forall i,j \neq i} (P^C_{i,j,d,t} + P^C_{j,i,d,t}) \tag{23}$$

$$\sum_{\forall g} P^G_{g,d,t}\mathcal{N}_{g,i} - \sum_{\forall j}(P^C_{i,j,d,t}) - P^D_{i,d,t} = 0 \tag{24}$$

$$\sum_{\forall g} Q^G_{g,d,t}\mathcal{N}_{g,i} - \sum_{\forall j}(Q^C_{i,j,d,t}) - Q^D_{i,d,t} = 0 \tag{25}$$

$$V^{min}_i \leq V_{i,d,t} \leq V^{max}_i \tag{26}$$

$$-\pi/2 \leq \delta_{i,d,t} \leq \pi/2 \tag{27}$$

$$P^{Gmin}_g \leq P^G_{g,d,t} \leq P^{Gmax}_g \tag{28}$$

$$Q^{Gmin}_g \leq Q^G_{g,d,t} \leq Q^{Gmax}_g \tag{29}$$

$$\begin{aligned} P^C_{i,j,d,t} = G^{CN}_{i,j,d,t}V^2_{i,d,t} - G^{CN}_{i,j,d,t}V_{i,d,t}V_{j,d,t}\cos\delta_{ij,d,t} \\ -B^{CN}_{i,j,d,t}V_{i,d,t}V_{j,d,t}\sin\delta_{ij,d,t} \end{aligned} \tag{30}$$

$$\begin{aligned} Q^C_{i,j,d,t} = -B^{CN}_{i,j,d,t}V^2_{i,d,t} + B^{CN}_{i,j,d,t}V_{i,d,t}V_{j,d,t}\cos\delta_{ij,d,t} \\ -G^{CN}_{i,j,d,t}V_{i,d,t}V_{j,d,t}\sin\delta_{ij,d,t} \end{aligned} \tag{31}$$

$$(P^C_{i,j,d,t})^2 + (Q^C_{i,j,d,t})^2 \leq (S^{max}_{i,j,t})^2 \tag{32}$$

Faulted operation (added SFCLs):

$$\sum_{\forall r} e_{l,r,t} \leq \varphi_{l,t} \tag{33}$$

$$\sum_{\forall x} f_{l,x,t} \leq \varphi_{l,t} \tag{34}$$

$$\sum_{\forall r} v_{g,r,t} \leq 1 \tag{35}$$

$$\sum_{\forall x} w_{g,x,t} \leq 1 \tag{36}$$

$$e_{l,r,t} \geq e_{l,r,t-1} \tag{37}$$

$$f_{l,x,t} \geq f_{l,x,t-1} \tag{38}$$

$$v_{g,r,t} \geq v_{g,r,t-1} \tag{39}$$

$$w_{g,x,t} \geq w_{g,x,t-1} \tag{40}$$

$$G^{PLS}_{i,j,t} = \sum_{\forall l,r,x} (G^{PLSR}_{l,r}e_{l,r,t} + G^{PLSX}_{l,x}f_{l,x,t})\varpi_{l,i,j} \tag{41}$$

$$B^{PLS}_{i,j,t} = \sum_{\forall l,r,x} (B^{PLSR}_{l,r}e_{l,r,t} + B^{PLSX}_{l,x}f_{l,x,t})\varpi_{l,i,j} \tag{42}$$

$$\begin{aligned} G^{CF}_{i,j,t} = \sum_{l \in \Omega_{LC}} G^L_l \varphi_{l,t}\varpi_{l,i,j} \\ + \sum_{\forall l,q}(G^{min}_{l,q} + G^{max}_{l,q})\psi_{l,q,t}\varpi_{l,i,j} + G^{PLS}_{i,j,t} \end{aligned} \tag{43}$$

$$\begin{aligned} B^{CF}_{i,j,t} = \sum_{l \in \Omega_{LC}} B^L_l \varphi_{l,t}\varpi_{l,i,j} \\ + \sum_{\forall l,q}(B^{min}_{l,q} + B^{max}_{l,q})\psi_{l,q,t}\varpi_{l,i,j} + B^{PLS}_{i,j,t} \end{aligned} \tag{44}$$

$$G^{PGS}_{i,t} = \sum_{\forall g,r,x} (G^{PGSR}_{g,r}v_{g,r,t} + G^{PGSX}_{g,x}w_{g,x,t})\mathcal{N}_{g,i} \tag{45}$$

$$B^{PGS}_{i,t} = \sum_{\forall g,r,x} (B^{PGSX}_{g,x}w_{g,x,t} + B^{PGSR}_{g,r}v_{g,r,t})\mathcal{N}_{g,i} \tag{46}$$

$$Z^{Im}_{i,t} = Z^{0,Im}_i + \sum_{\forall m,n} \Delta Z^{L,Im}_{i,m,n,t} + \sum_{\forall m} \Delta Z^{G,Im}_{i,m,t} \tag{47}$$

$$\Delta Z^{L,Im}_{i,m,n,t} = \frac{\left\{ \begin{matrix} A^{Im}_{i,m,n}G^{CF}_{m,n,t} + A^{Re}_{i,m,n}B^{CF}_{m,n,t} + \\ (A^{Im}_{i,m,n}B^{Re}_{m,n} - A^{Re}_{i,m,n}B^{Im}_{m,n})\left({G^{CF}_{m,n,t}}^2 + {B^{CF}_{m,n,t}}^2\right) \end{matrix} \right\}}{\left\{ \begin{matrix} 1 + 2B^{Re}_{m,n}G^{CF}_{m,n,t} - 2B^{Im}_{m,n}B^{CF}_{m,n,t} + \\ \left({B^{Re}_{m,n}}^2 + {B^{Im}_{m,n}}^2\right)\left({G^{CF}_{m,n,t}}^2 + {B^{CF}_{m,n,t}}^2\right) \end{matrix} \right\}} \tag{48}$$

$$\Delta Z^{G,Im}_{i,m,t} = \frac{\left\{ \begin{matrix} C^{Im}_{i,m} + (C^{Im}_{i,m}D^{Re}_m - C^{Re}_{i,m}D^{Im}_m)G^{PGS}_{m,t} \\ -(C^{Re}_{i,m}D^{Re}_m + C^{Im}_{i,m}D^{Im}_m)B^{PGS}_{m,t} \end{matrix} \right\}}{\left\{ \begin{matrix} 1 + 2D^{Re}_m G^{PGS}_{m,t} - 2D^{Im}_m B^{PGS}_{m,t} \\ +\left({D^{Re}_m}^2 + {D^{Im}_m}^2\right)\left({G^{PGS}_{m,t}}^2 + {B^{PGS}_{m,t}}^2\right) \end{matrix} \right\}} \tag{49}$$

$$I^{SC}_{i,d,t} = V_{i,d,t}/Z^{im}_{i,t} \leq I^{SC,max}_i \ . \tag{50}$$

The objective function in (12) includes investment cost (C_I) and operation cost (C_{OP}). The first and second terms in (13) represent the cost of building new lines and TCSCs, respectively. The 3rd and 4th terms are investment cost of resistive and inductive SFCL modules, respectively, installed in existing and new lines. Similarly, the 5th and 6th terms are related to generator SFCLs. The two terms in (14) indicate the operation cost of power generation and energy losses over the planning horizon. We have considered a number of demand levels obtained using the *k*-means clustering technique [13]. By this technique, the hourly load profile of each bus, consisting of 8760 hourly demands per year, is categorized into a predefined number of clusters, where the centroid of each cluster gives the cluster load level, and the number of hours in each cluster gives its duration. In this way, the obtained cluster load levels represent the whole year, while a significantly lower number of load values (compared to 8760 hourly demands) are considered. Cost terms in (13)-(14) are converted to net present values.

Constraints in (15)-(16) guarantee that if a candidate line or a TCSC is constructed or installed at a time period, it is also available at subsequent time periods. Equation (17) allows installing TCSC in only selected lines. It also guarantees that only a specific TCSC compensation level is selected in each time interval. This is due to the fact that the TCSC compensation level varies with the load profile. The left-hand and right-hand side summations in (18)-(19) represent the minimum and maximum, respectively, parallel equivalent conductance/susceptance of a TCSC to be installed in line l at time t. The resulting time-dependent admittance of transmission corridors is given by (20)-(21), where the first summation is from all lines (existing and new) and the second one is from installed TCSCs. $\varpi_{l,i,j}$ is used to convert a line-based index to a bus-based index. Note that since the impedance of SFCLs is nearly zero in normal operation, it is not considered in (20)-(21). Dynamic ratings of corridors are given by (22), where TCSCs are represented as parallel paths for power flow as shown in Fig. 2(b). Network power losses are given by (23). Note that network power losses, which are minimized as a part of the operation cost in (14), usually have a small contribution compared with the generation cost – the first term in (14). Active and reactive power balances per bus are enforced by (24) and (25). Operational limits of bus voltages and generator outputs are imposed by (26)-(27) and (28)-(29), respectively. It is noted that voltage magnitudes are bounded to vary within their limits and not optimized in the proposed TEP model. Time-dependent power flows of transmission corridors (through existing and new lines) are calculated using (30)-(31) ($\delta_{ij,d,t} = \delta_{i,d,t} - \delta_{j,d,t}$). The apparent power of transmission corridors is constrained by (32), which depends on existing and candidate lines as well as on TCSCs.

Constraints (33)-(34) allow installing modules of resistive and inductive SFCLs in selected lines. It also guarantees that only a specific number of modules of resistive/inductive SFCLs is selected. Similarly, (35)-(36) ensures the same for generator SFCLs. Constraints (37)-(40) imply that if a number of SFCL modules are placed at time period t, they are available in subsequent time periods.

The equivalent parallel admittance, which is added to corridor ij due to line SFCLs, is given by (41)-(42). Resistive and inductive SFCLs are expressed in impedances, not admittances, as they are installed in series with a line. However, we convert them to their parallel equivalent admittances as expressed by (1). If a purely resistive or inductive line SFCL is converted to its equivalent parallel admittance, it results in a complex-valued admittance. For instance, when a purely inductive SFCL $\boldsymbol{Z_{L1}^{SLS}} = jX$ is converted to its equivalent parallel admittance by (1), it produces the parallel complex-valued admittance $\boldsymbol{Y_{L1}^{PLS}} = G_{L1}^{PLSX} + jB_{L1}^{PLSX}$ as shown in Fig. 2(b). Consequently, the conductance/susceptance that is added in parallel to transmission corridors in (41)-(42) comes from both resistive and inductive SFCLs. Thus, the first and second terms in (41)-(42) result from the resistive and inductive SFCLs, respectively. The increment in admittance of transmission corridor ij at time t due to adding new lines, TCSCs, and SFCLs is given by (43)-(44). Similarly, the effect of generator SFCLs on self-admittance of buses is given by (45)-(46). Equation (47) updates Z_{BUS} diagonal element i after adding new components. The change in diagonal element i of Z_{BUS} as a result of adding new lines, TCSCs, and line SFCLs between buses m and n is given by (48), which is obtained from (7). Similarly, the effect of generator SFCLs on the diagonal element i of Z_{BUS} is given by (49) obtained from (11). The SC levels of all buses are calculated by (50) using the updated diagonal elements of Z_{BUS}. It is also limited to its permissible value $I_i^{SC,max}$ that is determined by the fault breaking capacity of existing switchgears.

B. Linearization of Nonlinear Constraints

In the proposed MINLP model (12)-(50), nonlinear constraints include (30)-(32) and (48)-(50). Note that these nonlinearities are mainly caused by the fact that impedances are variable in (30)-(31) due to adding TCSCs and updating of impedance matrix elements in (48)-(49) due to adding SFCLs. In view of the fact that existing power flow linearization techniques (such as those presented in [9], [24], [25]), convex models [22], or DC network models [1] are designed for constant branch admittances, they are not applicable here.

Power flow equations (30)-(31) are nonlinear functions of variables $X_1 = \{G_{i,j,d,t}^{CN},\, B_{i,j,d,t}^{CN},\, V_{i,d,t},\, V_{j,d,t},\, \delta_{ij,d,t}\}$. Similarly, impedance matrix change equations (48)-(49) are nonlinear functions of $X_2 = \{G_{m,n,t}^{CF}, B_{m,n,t}^{CF}\}$. Using the first order Taylor series expansion, these nonlinear functions are linearized around a base point X_0 as follows.

$$P_{i,j,d,t}^{C,LN} = P_{i,j,d,t}^{C}\big|_{X_{1,0}} + \sum_{\forall X_1} \frac{\partial P_{i,j,d,t}^{C}}{\partial X_1}\bigg|_{X_{1,0}} (X_1 - X_{1,0}) \quad (51)$$

$$Q_{i,j,d,t}^{C,LN} = Q_{i,j,d,t}^{C}\big|_{X_{1,0}} + \sum_{\forall X_1} \frac{\partial Q_{i,j,d,t}^{C}}{\partial X_1}\bigg|_{X_{1,0}} (X_1 - X_{1,0}) \quad (52)$$

$$\begin{aligned}&\Delta Z_{i,m,n,t}^{L,LN,Im} \\ &= \Delta Z_{i,m,n,t}^{L,Im}\big|_{X_{2,0}} + \sum_{\forall X_2} \frac{\partial \Delta Z_{i,m,n,t}^{L,Im}}{\partial X_2}\bigg|_{X_{2,0}} (X_2 - X_{2,0})\end{aligned} \quad (53)$$

$$\begin{aligned}&\Delta Z_{i,m,t}^{G,LN,Im} \\ &= \Delta Z_{i,m,t}^{G,Im}\big|_{X_{2,0}} + \sum_{\forall X_2} \frac{\partial \Delta Z_{i,m,t}^{G,Im}}{\partial X_2}\bigg|_{X_{2,0}} (X_2 - X_{2,0})\end{aligned} \quad (54)$$

where $X_{1,0}$ and $X_{2,0}$ are values of X_1 and X_2, respectively, at base point X_0; superscript *LN* indicates the linearized value of the nonlinear functions. Note that the accuracy of Taylor first order expansion is reasonable only around the base point. To improve accuracy, we later introduce a BD scheme to update the base point in order to minimize linearization errors.

To linearize quadratic constraint (32) to get an MILP model, we employ the technique proposed in [25] since it results in an acceptable linearization error. The feasible region constrained by $x^2 + y^2 \leq r^2$ represents the area inside a circle in the $x - y$ plane centered at the origin with radius r. This area can be approximated by a number of lines defining a polygon inside the circle at evenly spaced points. Line k is represented as $a_k x + b_k y = c_k r$, where a_k, b_k, and c_k are constants defining the slope and position of line k. The intersection of the areas $a_k x + b_k y \leq c_k r$ confined by these lines approximates the circle area. Thus, (32) is linearized using a set of linear constraints as:

$$a_k P_{i,j,d,t}^{C,LN} + b_k Q_{i,j,d,t}^{C,LN} \leq c_k S_{i,j,t}^{max}\ . \quad (55)$$

Also, nonlinear equation (50) can be rewritten as a linear one:

$$V_{i,d,t} \leq Z_{i,t}^{Im} I_i^{SC,max}\ . \quad (56)$$

Finally, the linearized MILP model of the proposed MINLP problem seeks to minimize (12) subject to:

$$P_{d,t}^{Loss} = \sum_{\forall i, j \neq i} \left(P_{i,j,d,t}^{C,LN} + P_{j,i,d,t}^{C,LN}\right) \quad (57)$$

$$\sum_{\forall g} P_{g,d,t}^{G} \mathcal{N}_{g,i} - \sum_{\forall j} \left(P_{i,j,d,t}^{C,LN}\right) - P_{i,d,t}^{D} = 0 \quad (58)$$

$$\sum_{\forall g} Q_{g,d,t}^{G} \mathcal{N}_{g,i} - \sum_{\forall j} \left(Q_{i,j,d,t}^{C,LN}\right) - Q_{i,d,t}^{D} = 0 \quad (59)$$

$$Z_{i,t}^{Im} = Z_i^{0,Im} + \sum_{\forall m,n} \Delta Z_{i,m,n,t}^{L,LN,Im} + \sum_{\forall m} \Delta Z_{i,m,t}^{G,LN,Im} \quad (60)$$

(13)-(22), (26)-(29), (33)-(47), (51)-(56). (61)

IV. Proposed Benders' Decomposition Scheme

A modified BD scheme is proposed below to minimize the linearization error of the MILP problem.

A. Master Problem (MP) of the Proposed BD Scheme

The MP is formulated as:

$$\min_{\varphi,\psi,e,f,v,w} f_{MP} \geq C_I \tag{62}$$

$$\text{s.t. (13), (15)-(17), (33)-(40).} \tag{63}$$

This MP is a small MILP problem to determine binary investment decisions.

B. Subproblem 1 (SP1) of the Proposed BD Scheme

This subproblem minimizes the operation cost subject to operational and security constraints. It is a linear programming (LP) problem:

$$\min_{P^G,Q^G} C_{OP} \tag{64}$$

$$\text{s.t. } Y = \bar{Y} \quad \rightarrow \quad \lambda^{SP1} \tag{65}$$

$$\text{(14), (57)-(61)} \tag{66}$$

where Y is the vector of binary variables that are set to the values obtained from the MP; λ^{SP1} are dual values.

C. Subproblem 2 (SP2) of the Proposed BD Scheme

SP2 determines the linearization errors and seeks their minimization. Thus, SP2 includes the nonlinear functions to calculate the exact nonlinear values. Hence, it is an NLP problem:

$$\begin{aligned}&\min_{\mu^P,\mu^Q,\mu^{ZL},\mu^{ZG}} \mu \\ &= \sum_{\forall i,j,d,t} \left(\mu^{P+}_{i,j,d,t} + \mu^{P-}_{i,j,d,t} + \mu^{Q+}_{i,j,d,t} + \mu^{Q-}_{i,j,d,t}\right) \\ &+ \sum_{\forall i,m,n,t} \left(\mu^{ZL+}_{i,m,n,t} + \mu^{ZL-}_{i,m,n,t}\right) + \sum_{\forall i,m,t} \left(\mu^{ZG+}_{i,m,t} + \mu^{ZG-}_{i,m,t}\right)\end{aligned} \tag{67}$$

$$\text{s.t. } Y = \bar{Y} \quad \rightarrow \quad \lambda^{SP2} \tag{68}$$

$$\text{(14), (30)-(31), (48)-(49), (57)-(61)} \tag{69}$$

$$P^{C,LN}_{i,j,d,t} - P^{C}_{i,j,d,t} + \mu^{P-}_{i,j,d,t} - \mu^{P+}_{i,j,d,t} = 0 \tag{70}$$

$$Q^{C,LN}_{i,j,d,t} - Q^{C}_{i,j,d,t} + \mu^{Q+}_{i,j,d,t} - \mu^{Q-}_{i,j,d,t} = 0 \tag{71}$$

$$\Delta Z^{L,LN,im}_{i,m,n,t} - \Delta Z^{L,im}_{i,m,n,t} + \mu^{ZL-}_{i,m,n,t} - \mu^{ZL+}_{i,m,n,t} = 0 \tag{72}$$

$$\Delta Z^{G,LN,im}_{i,m,t} - \Delta Z^{G,im}_{i,m,t} + \mu^{ZG-}_{i,m,t} - \mu^{ZG+}_{i,m,t} = 0 \tag{73}$$

where λ^{SP2} are dual values. Linearization errors are calculated by (70)-(73) as the differences between the linearized and the nonlinear functions using positive slack variables. In other words, $P^{C}_{i,j,d,t}$, $Q^{C}_{i,j,d,t}$, $\Delta Z^{L,im}_{i,m,n,t}$, and $\Delta Z^{G,im}_{i,m,t}$ are considered actual values and linearization errors are measured using slack variables as the differences between these actual values and the results obtained from the linearized model including $P^{C,LN}_{i,j,d,t}$, $Q^{C,LN}_{i,j,d,t}$, $\Delta Z^{L,LN,im}_{i,m,n,t}$, and $\Delta Z^{G,LN,im}_{i,m,t}$. If the value obtained for the objective function of SP2, denoted by $\bar{\mu}$, is zero, linearization errors are null. Otherwise, an infeasibility cut is generated to be added to MP as:

$$\bar{\mu} + \sum \lambda^{SP2}(Y - \bar{Y}) \leq 0 \ . \tag{74}$$

A feasibility cut is also generated to be added to the MP in the next iteration:

$$f_{MP} \geq C_I + \overline{C_{OP}} + \sum \lambda^{SP1}(Y - \bar{Y}) \tag{75}$$

Algorithm 1: Proposed BD Scheme.

1. Solve MP and obtain optimal investment decisions $\bar{Y} = Y^*$ and $\overline{f_{MP}}$.
2. Update the BD lower bound as $LB = \overline{f_{MP}}$.
3. Solve SP1 to obtain its optimal objective function $\overline{C_{OP}}$.
4. Construct feasibility cut to be added to MP.
5. Update the BD upper bound as $UB = \overline{f_{MP}} + \overline{C_{OP}}$.
6. Update base point X_0 of linearization using the solution obtained from SP1.
7. Re-linearize nonlinear functions around the updated base point X_0.
8. Solve SP2 to minimize linearization errors.
9. If SP2 objective function $\bar{\mu}$ is not zero, construct infeasibility cut to be added to MP.
10. If LB and UB are close enough together and linearization error $\bar{\mu}$ is small enough, stop.
11. Go to step 1.

where $\overline{C_{OP}}$ is the optimal operation cost obtained from SP1. Equations (74) and (75) steer the BD solution to a point where the upper and lower bounds are sufficiently close and the linearization errors are minimized at the same time.

D. Proposed BD Scheme

The proposed BD scheme, described in Algorithm 1, moves linearization errors to zero. To do this, it updates the base point X_0 of Taylor expansion as indicated in step 6 of Algorithm 1. Then, (51)-(54) are re-linearized in Step 7. This procedure moves X_0 towards optimality and thus reduces the linearization errors over BD iterations. This way, Taylor series expansion becomes increasingly accurate. Once SP2 objective function becomes zero, an optimal solution is obtained for the original MINLP problem. A globally optimal solution is ensured for the MP and SP1 since they are MILP and LP problems, respectively. For SP2, its solution evolves over successive iterations. The convergence of the proposed BD scheme is similar to that of a standard BD scheme, which has already been discussed in the literature [26]. In addition, the results reported in Section V clearly illustrate the convergence of the proposed BD scheme on different case studies. Note that the original MINLP model may not be tractable if it is directly solved using available solvers.

V. Extending the Proposed Model to Include Uncertainties

It is worth noting that the current paper presents a deterministic version of the proposed model for clarity and better presentation of the underlying ideas. However, it can be extended to incorporate TEP problem uncertainties, such as uncertainties in load forecasts and investment costs [27]. For this purpose, we can employ stochastic programming (SP) approaches that model uncertainties using sampled scenarios [28], robust optimization (RO) approaches that model uncertainties using bounded intervals [28], and information gap decision theory (IGDT) approaches that model uncertainties using envelope bounds [27]. However, all of these approaches require a deterministic model of the TEP problem and start from it to characterize uncertainties.

To extend the proposed deterministic TEP model to consider uncertainties constitutes future research work. In addition, by considering the uncertainties, the computation burden of the problem usually increases. The proposed Benders decomposition-based solution approach, which significantly decreases the computation burden of the problem as shown in the next section, can be effectively used to cope with the increased computation burden due to modeling uncertainties.

Additionally, the reliability of a power system can be affected by adding new transmission components, such as lines, TCSCs, and SFCLs. For instance, by selecting transmission components with higher availability or lower forced outage rate (FOR) for critical transmission corridors, we can decrease the reliability index of expected energy not supplied (EENS) and thus improve the power system reliability. However, power system reliability is studied using the FOR of the system components [29] and thus it is related to the uncertainties of availability of components. By considering component availability uncertainties in the proposed TEP approach (which are discrete uncertainty sources and can be modeled, for instance, by scenario-based methods [28]), the proposed approach can model and optimize power system reliability.

VI. Case Studies and Numerical Results

The proposed method is tested on the IEEE 39-bus and 118-bus test systems. TCSCs are considered with a maximum of seven compensation modules, the optimal number of which is decided by the model. Also, hybrid SFCLs are assumed with up to 10 series R and X modules ($|\Omega_r| = |\Omega_x| = 10$), the optimal number and location of which are selected by the model. The nominal interrupting rating of circuit breakers is assumed to be $I_i^{SC,max} = 30$ kA [3]. The discount rate and energy cost are considered to be $\gamma = 10\%$ and $\pi_t = 40$ \$/MWh, respectively [30], [31]. Investment costs of TCSCs and lines are assumed to be \$22000/MVA and \$2000/MW-mile, respectively [1]. Network data, such as line impedances, loads, and generations, have been obtained from [32]. Investment cost of each SFCL module is assumed to be M\$0.189. Two candidate lines are considered in each existing corridor with the same specifications as the existing lines. Load annual growth rate is considered 5%. Two planning horizons of $|\Omega_T| = 8$ and 10 years are considered to examine the proposed methods. These two planning horizons are selected to analyze the effect of SFCLs on the solution feasibility. The number of linear segments to approximate the circle in (55) is 12 as such number results in a good balance between accuracy and computation time. The proposed model is implemented in GAMS [33] using a 2.8 GHz core i7 personal computer. Solvers GUROBI and CONOPT are used to solve the MILP and NLP models, respectively.

A. IEEE 39-Bus Test System: Joint Planning of Lines and TCSCs without SFCLs

The methods TEP and TEP + TCSC are examined first. The results obtained are shown in Table I, where the two planning horizons of 8 and 10 years are indicated by (a) and (b), respectively. TEP with planning horizon (a) plans lines 2-3 and 22-35 in year 8. TEP + TCSC plans no line; instead, it plans three TCSCs in the last year of case (a). Specifically, the first TCSC "(2-3).C7" is planned at year 8 in line 2-3 with seven compensation modules (C7). Note that TCSCs provide an alternative approach, as compared to building new lines, to increase the capacity of transmission corridors and to meet prospective demand levels. TEP + TCSC results in a cost of 0.589M\$, which is lower than the 3.017M\$ TEP cost. This implies that TEP + TCSC provides a cost-effective solution with respect to TEP. The results of TEP (a) and TEP + TCSC (a) in Table I are feasible without using SFCLs. Note that power loss and generation cost terms in (14) are 1.2% and 98.8% of the operation cost, respectively, implying that generation cost dominates total operation cost. All bus voltage magnitudes obtained by the proposed TEP approach are within the allowable ranges specified in (26).

To evaluate the voltage stability characteristics of TEP solutions, we have used the continuation power flow (CPF) method to determine the voltage stability margin (VSM) based on eigenvalue analysis. We have applied the CPF method and monitored the eigenvalues of the power flow Jacobian matrix for singularity. The point in which the Jacobian matrix becomes singular (at least one zero eigenvalue) indicates the loadability margin or VSM of the system [34]. A larger VSM implies a

Table I. Planned components by different methods with Two planning horizons without using SFCLs

Method	Planned components	Cost (M\$)
TEP (a)	**Lines in Y8:** 2-3, 22-35.	3.017
TEP + TCSC (a)	**TCSCs in Y8:** (2-3).C7, (4-5).C4, (13-14).C2.	0.589
TEP (b)	No feasible solution	---
TEP + TCSC (b)	No feasible solution	---

Yn: year n; (i-j).Cm: TCSC at line i-j with m compensation modules.

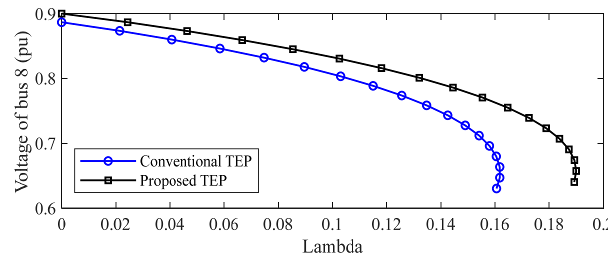

Fig. 3. Voltage stability margin for the conventional TEP solution and proposed TEP solution in case (a) of Table I.

Table II. Planned components by different methods using SFCLs with 10-year Planning Horizon

Method	Planned components	Cost (M\$)
TEP + SFCL (b)	**Lines in Y8:** 2-3, 4-5; **Lines in Y9:** 4-14, 10-13, 13-14, 17-18, 19-33, 22-35, 26-27; **Lines in Y10:** 3-4, 3-18, 15-16, 16-19, 16-24, 20-34, 21-22, 23-24, 23-36, 25-26, 25-37, 29-38.	30.113
	SFCLs in Y10: (26-28).R1.	0.189
TEP + TCSC + SFCL (b)	**Lines in Y9:** 2-3, 4-5; **Lines in Y10:** 10-13, 13-14, 19-33, 22-35.	6.242
	TCSCs in Y8: (2-3).C7, (4-5).C7; **TCSCs in Y9:** (10-13).C7, (13-14).C7; **TCSCs in Y10:** (26-27).C3, (13-14).C6.	1.189
	SFCLs at Y10: (5-6).R1.	0.189

(i-j).Rm: SFCL at line i-j with m resistive modules.

Table III. Results of the proposed BD solution method

Nonlinear equation	Linearization MMAPE (%)					
	Iter 1	Iter 2	Iter 3	Iter 4	Iter 5	Iter 6
Line active power	8.04	2.04	0.04	0.02	0.00	0.00
Line reactive power	9.14	6.49	3.57	1.25	0.09	0.00
Change in Z_{BUS} elements	11.26	8.51	3.48	1.97	0.93	0.00
Overall	9.56	5.48	2.04	0.96	0.07	0.00

Table IV. Elapsed times by iterations

Iteration	1	2	3	4	5	6	Total
Elapsed time (sec)	281.5	211.3	142.9	118.6	77.1	34.6	866

more stable system from the voltage stability viewpoint. The results of this study for the conventional TEP and the proposed TEP solutions in case (a) of Table I are shown in Fig. 3. In this figure, the horizontal axis represents the parameter λ of the CPF, which indicates the increase in the active and reactive loads of buses. Details of the CPF method can be found in [32]. Out of all buses, bus 8 in our simulations has the lowest voltage magnitude at the voltage stability boundary in both conventional and proposed TEP solutions and thus, the voltage at this bus has been plotted in Fig. 3. The nose point of the curves in this figure represents the voltage stability border, beyond which the power system becomes unstable [34]. In the simulations illustrated in Fig. 3, the proposed TEP solution results in $\lambda = 0.1893$, whereas the conventional TEP solution results in $\lambda = 0.1611$. This indicates that the proposed TEP enhances the VSM by 17.5% in this case. Considering other advantages of the proposed TEP method, such as its lower total cost as reported in Table I, we can conclude that the proposed TEP outperforms the conventional TEP.

As indicated in Table I, for the planning horizon of 10 years in case (b), both methods TEP and TEP + TCSC fail to provide a feasible solution. This is due to the fact that more lines/TCSCs are needed to meet the load demand in a longer planning horizon, especially in the last years. The increased number of lines and TCSCs, in turn, reduces the impedance of transmission corridors resulting in increased SC levels at buses. Since SC limits are enforced, it is not possible to meet the demand and, at the same time, to keep the SC levels at their permitted ranges in case (b). In fact, the 8-year period is the longest planning horizon in which a feasible TEP solution can be found without SFCLs. Note that the infeasibility in the 10-year planning horizon case is not related to the system size; it happens due to violation of SC levels of buses as expressed in (50) in the last years of the planning horizon. SFCLs provide a solution for this problem. They make it possible to control SC levels and to meet the load growth simultaneously. If SFCLs are not considered, an alternative is to reinforce the SC level of the components of existing substations (switchgears, cables, generators, etc.). However, this reinforcement may not be a practical solution because it needs high investment and power interruptions during the upgrading.

B. IEEE 39-Bus Test System: Joint Planning of Lines and TCSCs with SFCLs

Results with SFCLs are shown in Table II for case (b). If SFCLs are considered in TEP, the method TEP + SFCL plans 2, 7, and 12 lines in years 8, 9, and 10, respectively, to meet the demand. In addition, one SFCL is planned in year 10 in line 26-28 with one resistive module (R1). As a result, not only the load is supplied, but also SC levels are controlled by the SFCL. Although the network has a dominating inductance as compared with its resistance, a resistive SFCL is selected. From the cost point of view, the SFCL costs only 0.189M$, which is very small as compared with 30.113M$ network expansion planning cost (about 0.63%). This implies that SFCLs provide a cost-effective solution to the SC-constrained TEP. Regarding the next method of Table II (TEP + TCSC + SFCL), six lines are planned in years 9 and 10. Also, six TCSCs are planned in years 8-10. A SFCL with one resistive module is also planned in year 10. The cost of SFCL (0.189M$) is again acceptable (about 2.5%) if compared with the total cost of network expansion (6.242 + 1.189 = 7.431M$). The cost terms of both methods are depicted in Fig. 4 as stacked bars. For clarity, the values of bar stacks are also added beside stacks. If the two methods are compared from the total cost point of view, the first method TEP + SFCL leads to 30.113 + 0.189 = 30.302M$, whereas the second method TEP + TCSC + SFCL results in 6.242 + 1.189 + 0.189 = 7.620M$ (about 75% lower). This finding indicates that it is advantageous to employ SFCLs in TEP with TCSCs.

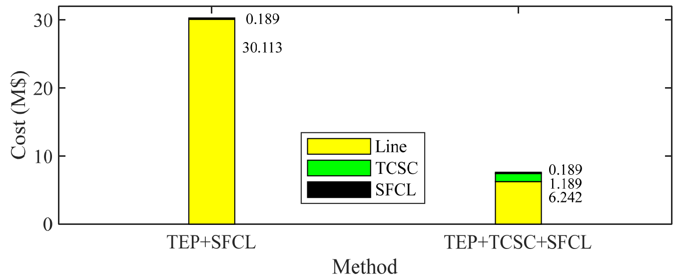

Fig. 4. Cost components of the two methods in the 10-year planning horizon.

C. IEEE 39-Bus Test System: Moving Linearization Errors to Zero

The linearization error of the proposed solution method is measured by the modified mean absolute percentage error (MMAPE) index [35]:

$$MMAPE = \frac{1}{n} \times \sum_{i=1}^{n} \frac{|x_i^a - x_i^e|}{|\overline{x^a}|} \tag{76}$$

where n is the number of values; x_i^a and x_i^e are the i^{th} actual and estimated values obtained using the original nonlinear and linearized functions, respectively; $\overline{x^a}$ is the average of actual values. Note that $\overline{x^a}$ is used in the denominator in (76) to avoid the problem caused by very small or zero values of x_i^a [35].

The results of the proposed BD scheme with re-linearization are provided in Table III, where linearization errors are given for individual linearized functions and also in total. The overall error in this table is calculated by including all error elements in a single error vector and computing MMAPE for that single error vector. The overall MMAPE is 9.56% after the first iteration. By minimizing the linearization errors in SP2 and adding infeasibility Benders cuts to the MP, the linearization errors ultimately approach zero (with a two-digit accuracy). This implies that the linearization errors are effectively reduced by re-linearizing nonlinear functions around the updated base point over Benders iterations. At the same time, the upper and lower bounds of the BD solution get close to each other (within 1% optimality gap) as a result of enforcing the feasibility Benders cuts obtained from SP1 in the MP. Elapsed times for each iteration are presented in Table IV. The total elapsed time to solve the problem for the IEEE 39-bus test system was 14 minutes and 26 seconds (866 seconds). Although computation time may not be as critical as linearization errors for the planning problem, it confirms the tractability of the proposed model.

The original MINLP form of the proposed model is a much more complicated optimization problem than the linearized one due to the complexity of its nonlinear constraints, including highly nonlinear power flow equations (with variable line admittances) and change in the impedance matrix. We tried to directly solve the original MINLP problem with available MINLP

TABLE V. PLANNED COMPONENTS BY THE TEP + TCSC + SFCL METHOD ON THE IEEE 118-BUS TEST SYSTEM

Item	Time and location
Line	**Y6:** 91-92**; Y7:** 68-116, 89-90; **Y10:** 9-10, 42-49, 47-69.
TCSC	**Y4:** (68-116).C6; **Y9:** (8-9).C7, (15-17).C7, (34-37).C7, (37-38).C7, (37-39).C3, (68-116).C4; **Y10:** (1-3).C3, (4-5).C6, (5-6).C6, (8-30).C2, (17-18).C4, (20-21).C1, (23-32).C3, (37-40).C4, (39-40).C1, (40-41).C1, (74-75).C2, (78-79).C1, (91-92).C7, (91-92).C4.
SFCL	**Y6:** (49).R10, (103).R10, (111).R10; **Y10:** (61-64).X1.

(i-j).Xm: SFCL at line i-j with m inductive modules; (n).Rm: SFCL at generator n with m resistive modules.

solvers in GAMS. However, all of these solvers failed to solve the original MINLP problem for this case study even after 12 hours of computing time. On the contrary, the proposed BD solution method finds a solution that matches the original MINLP problem due to a zero linearization error in a reasonable computation time. The high computational efficiency of the proposed solution method comes from linearizing the highly nonlinear constraints and decomposing the original problem into the smaller problems MP, SP1, and SP2.

D. IEEE 118-Bus Test System: Joint Planning of Lines, TCSCs and SFCLs

This test system, the data of which can be found in [32], is selected to evaluate the scalability of the proposed model. The results of planning by the proposed model in its complete form (i.e., TEP + TCSC + SFCL) with a 10-year planning horizon are shown in Table V. As seen, the proposed model has planned 6 lines in years 6, 7, and 10. Also, it plans 21 TCSCs in years 4, 9, and 10 to reduce the number of required lines and to achieve a more cost-effective solution. Finally, it plans 3 resistive SFCLs on generators and 1 inductive SFCL on a line in years 6 and 10, respectively, to limit the SC levels of buses. The total cost of planning by the proposed TEP model is $55.751M with a major part of line cost. By these planned components, the load growth is supplied and all the TEP constraints, presented in Section III, are satisfied.

The total computing time of the proposed model for the IEEE 118-bus test system with a 10-year planning horizon is as 44 minutes and 8 seconds, which is a reasonable computing time for this planning problem. This computing time confirms the tractability of the proposed model in larger-scale systems, which is due to the Benders decomposition and linearization of the proposed solution method.

VII. CONCLUSIONS

In this paper, a framework is proposed for the joint planning of hybrid SFCLs, TCSCs, and transmission lines. Also, a BD solution method is proposed to minimize linearization errors. From the case study, we have found that 1) introducing TCSCs can significantly reduce TEP costs, 2) longer planning horizons without SFCLs may result in infeasibilities since adding more lines/TCSCs increases the SC level of buses, 3) SFCLs provide a cost-effective solution for SC-constrained TEP, and 4) while the original MINLP problem is not solvable in our case study, the proposed BD solution method finds an optimal solution in a reasonable computation time.

REFERENCES

[1] O. Ziaee, O. Alizadeh-Mousavi, and F. F. Choobineh, "Co-optimization of transmission expansion planning and TCSC placement considering the correlation between wind and demand scenarios," *IEEE Trans. Power Syst.*, vol. 33, no. 1, pp. 206–215, 2018.

[2] S. Nilsson *et al.*, "Application examples of the thyristor controlled series capacitor," in *Flexible AC Transmission Systems: FACTS, CIGRE Green Books*, Springer, Cham, 2019, pp. 1–59.

[3] S. Teimourzadeh and F. Aminifar, "MILP formulation for transmission expansion planning with short-circuit level constraints," *IEEE Trans. Power Syst.*, vol. 31, no. 4, pp. 3109–3118, 2016.

[4] S. Eckroad, "Superconducting Power Equipment: Technology Watch 2012," *EPRI, CA 2012. 1024190*, 2012.

[5] G. Didier, J. Lévêque, and A. Rezzoug, "A novel approach to determine the optimal location of SFCL in electric power grid to improve power system stability," *IEEE Trans. Power Syst.*, vol. 28, no. 2, pp. 978–984, 2013.

[6] EPRI and S. Eckroad, "Superconducting fault current limiters: technology watch 2009," CA, USA, 2009.

[7] S. Dehghan, N. Amjady, and A. J. Conejo, "A multistage robust transmission expansion planning model based on mixed binary linear decision rules - Part I," *IEEE Trans. Power Syst.*, vol. 33, no. 5, pp. 5341–5350, 2018.

[8] N. Amjady, A. Attarha, S. Dehghan, and A. J. Conejo, "Adaptive robust expansion planning for a distribution network with DERs," *IEEE Trans. Power Syst.*, vol. 33, no. 2, pp. 1698–1715, 2018.

[9] Z. Li, J. Yu, and Q. H. Wu, "Approximate linear power flow using logarithmic transform of voltage magnitudes with reactive power and transmission loss consideration," *IEEE Trans. Power Syst.*, vol. 33, no. 4, pp. 4593–4603, 2018.

[10] P. A. Trodden, W. A. Bukhsh, A. Grothey, and K. I. M. McKinnon, "Optimization-based islanding of power networks using piecewise linear AC power flow," *IEEE Trans. Power Syst.*, vol. 29, no. 3, pp. 1212–1220, 2014.

[11] H. Gharibpour, F. Aminifar, and M. Haji Bashi, "Short-circuit-constrained transmission expansion planning with bus splitting flexibility," *IET Gener. Transm. Distrib.*, vol. 12, no. 1, pp. 217–226, 2018.

[12] Guk-Hyun Moon, Jaehee Lee, and Sung-Kwan Joo, "Integrated generation capacity and transmission network expansion planning with superconducting fault current limiter (SFCL)," *IEEE Trans. Appl. Supercond.*, vol. 23, no. 3, Article no 5000510, 2013.

[13] M. Esmaili, M. Ghamsari-Yazdel, N. Amjady, and A. J. Conejo, "Short-circuit constrained power system expansion planning considering bundling and voltage levels of lines," *IEEE Trans. Power Syst.*, vol. 35, no. 1, pp. 584–593, 2020.

[14] G. Didier and J. Lévêque, "Influence of fault type on the optimal location of superconducting fault current limiter in electrical power grid," *Int. J. Electr. Power Energy Syst.*, vol. 56, pp. 279–285, 2014.

[15] P. T. Ngoc and J. G. Singh, "Short circuit current level reduction in power system by optimal placement of fault current limiter," *Int. Trans. Electr. Energy Syst.*, vol. 27, no. 12, pp. 1–16, 2017.

[16] P. Yu, B. Venkatesh, A. Yazdani, and B. N. Singh, "Optimal location and sizing of fault current limiters in mesh networks using iterative mixed integer nonlinear programming," *IEEE Trans. Power Syst.*, vol. 31, no. 6, pp. 4776–4783, 2016.

[17] H.-T. Yang, W.-J. Tang, and P. R. Lubicki, "Placement of fault current limiters in a power system through a two-stage optimization approach," *IEEE Trans. Power Syst.*, vol. 33, no. 1, pp. 131–140, 2018.

[18] A. Elmitwally, E. Gouda, and S. Eladawy, "Restoring recloser-fuse coordination by optimal fault current limiters planning in DG-integrated distribution systems," *Int. J. Electr. Power Energy Syst.*, vol. 77, pp. 9–18, 2016.

[19] H. T. Roh and J. W. Lee, "Residential demand response scheduling with multiclass appliances in the smart grid," *IEEE Trans. Smart Grid*, vol. 7, no. 1, pp. 94–104, 2016.

[20] A. J. Conejo, E. Castillo, R. Mínguez, and R. García-Bertrand, *Decomposition techniques in mathematical programming: Engineering and science applications*. Berlin: Springer, 2006.

[21] M. Khanabadi, H. Ghasemi, and M. Doostizadeh, "Optimal transmission switching considering voltage security and N-1 contingency analysis," *IEEE Trans. Power Syst.*, vol. 28, no. 1, pp. 542–550, 2013.

[22] M. Bynum, A. Castillo, J. P. Watson, and C. D. Laird, "Tightening McCormick relaxations toward global solution of the ACOPF problem," *IEEE Trans. Power Syst.*, vol. 34, no. 1, pp. 814–817, 2019.

[23] J. J. Grainger and W. D. Stevenson, *Power system analysis*. Singapore: McGraw-Hill, 1994.

[24] X. Zhang, K. Tomsovic, and A. Dimitrovski, "Security constrained multi-stage transmission expansion planning considering a continuously variable series reactor," *IEEE Trans. Power Syst.*, vol. 32, no. 6, pp. 4442–4450, 2017.

[25] M. Tavakoli Bina and T. Akbari, "Approximated MILP model for AC transmission expansion planning: global solutions versus local solutions," *IET Gener. Transm. Distrib.*, vol. 10, no. 7, pp. 1563–1569, 2016.

[26] A. Ghanbari-Firouzabadi, A. Pirayesh, and M. Esmaili, "Efficient period elimination Benders decomposition for network-constrained AC unit commitment," *IET Gener. Transm. Distrib.*, vol. 13, no. 10, pp. 1802–1810, 2019.

[27] S. Dehghan, A. Kazemi, and N. Amjady, "Multi-objective robust transmission expansion planning using information-gap decision theory and augmented ε-constraint method," *IET Gener. Transm. Distrib.*, vol. 8, no. 5, pp. 828–840, 2014.

[28] S. Dehghan, N. Amjady, and A. J. Conejo, "Reliability-Constrained Robust Power System Expansion Planning," *IEEE Trans. Power Syst.*, vol. 31, no. 3, pp. 2383–2392, 2016.

[29] R. N. Allan and R. Billinton, *Reliability evaluation of power systems*, 2nd ed. New York: Springer US, 1996.

[30] H. Saboori and R. Hemmati, "Considering carbon capture and storage in electricity generation expansion planning," *IEEE Trans. Sustain. Energy*, vol. 7, no. 4, pp. 1371–1378, 2016.

[31] A. H. Dominguez, L. H. MacEdo, A. H. Escobar, and R. Romero, "Multistage security-constrained HVAC/HVDC transmission expansion planning with a reduced search space," *IEEE Trans. Power Syst.*, vol. 32, no. 6, pp. 4805–4817, 2017.

[32] R. D. Zimmerman, C. E. Murillo-Sanchez, R. J. Thomas, C. E. Murillo-Sánchez, and R. J. Thomas, "MATPOWER: Steady-state operations, planning, and analysis tools for power systems research and education," *IEEE Trans. Power Syst.*, vol. 26, no. 1, pp. 12–19, 2011.

[33] R. E. E. Rosenthal, M. R. Bussieck, and A. Meeraus, *General algebraic modeling system (GAMS)*. Washington, DC, USA: GAMS Development Corporation, www.gams.com, 2019.

[34] M. Esmaili and M. Ghamsari-Yazdel, "Voltage Stability-Constrained Optimal Simultaneous Placement of PMUs and Channels Enhancing Measurement Reliability and Redundancy," *IEEE Power Energy Technol. Syst. J.*, vol. 4, no. 2, pp. 32–39, 2017.

[35] O. Abedinia, N. Amjady, and H. Zareipour, "A new feature selection technique for load and price forecast of electrical power systems," *IEEE Trans. Power Syst.*, vol. 32, no. 1, pp. 62–74, 2017.